

# Barriers to Folding of the Transmembrane Domain of the *Escherichia coli* Autotransporter Adhesin Involved in Diffuse Adherence<sup>†</sup>

Jesper E. Mogensen,<sup>‡</sup> Damini Tapadar,<sup>§</sup> M. Alexander Schmidt,<sup>§</sup> and Daniel E. Otzen<sup>\*,‡</sup>

Department of Life Sciences, Aalborg University, Sohngaardsholmsvej 49, DK-9000 Aalborg, Denmark, and Institut für Infektiologie, Zentrum für Molekularbiologie der Entzündung (ZMBE), Westfälische Wilhelms-Universität Münster, Von-Esmarch-Strasse 56, D-48149 Münster, Germany

Received November 26, 2004; Revised Manuscript Received January 20, 2005

**ABSTRACT:** Adhesin involved in diffuse adherence (AIDA) is an autotransporter protein that confers the diffuse adherence phenotype to certain diarrheagenic *Escherichia coli* strains. It consists of a 49 amino acid signal peptide, a 797 amino acid passenger domain, and a 440 amino acid  $\beta$ -domain integrated in the outer membrane. The  $\beta$ -domain consists of two parts: the  $\beta_1$ -domain, which is predicted to form two  $\beta$ -strands on the bacterial cell surface, and the  $\beta_2$ -domain, which constitutes the transmembrane domain. We here present a detailed biophysical analysis of the AIDA  $\beta$ -domain addressing its refolding properties and its different conformational states and their stability. We find that the  $\beta_2$ -domain in solution can fold only when the  $\beta_1$ -domain is present and only with 50% efficiency. However, 100% refolding of the  $\beta_2$ -domain, with or without the  $\beta_1$ -domain, can be achieved in the presence of a solid support. Folding can only take place above the cmc of the detergent used, but the refolded state is retained if diluted below the cmc, revealing a kinetic barrier to dissociation of the detergent molecules from the folded protein. Refolding attempts of the  $\beta_2$ -domain in the absence of a solid support result in the formation of an oligomeric misfolded state both in the absence and in the presence of detergent. Despite being misfolded, these states unfold cooperatively with a  $T_m \approx 70$  °C. The refolded protein in the nonionic detergent octylpolyoxyethylene (oPOE) can only be thermally unfolded in the presence of SDS. The linear relationship between SDS mole fraction and unfolding temperature,  $T_m$ , predicts a  $T_m$  of  $112.9 \pm 1.2$  °C for the  $\beta_2$ -domain and  $132.7 \pm 12.2$  °C for the entire  $\beta$ -domain in pure oPOE. Thus, the  $\beta_1$ -domain also stabilizes the  $\beta_2$ -domain. In conclusion, our data show that the in vitro refolding of the AIDA  $\beta$ -domain is critically dependent on a solid support, suggesting that in vivo specific biological factors may assist in folding the protein correctly into the outer membrane to avoid the formation of stably misfolded conformations.

Outer membrane proteins (OMPs)<sup>1</sup> are integral membrane proteins that are found in the outer membranes of Gram-negative bacteria, mycobacteria, mitochondria, and chloroplasts (2, 3). In Gram-negative bacteria they constitute up to 2–3% of the genome (4). The three-dimensional structure

of the transmembrane domains of all bacterial members and some organellar members is composed of a  $\beta$ -barrel with an even number of  $\beta$ -strands (5). This structural motif is unique to OMPs as inner membrane proteins are composed of  $\alpha$ -helices that bundle together in the membrane (6). Despite the limited structural variability in OMPs, their functions are very diverse as they can be porins, transporters, protein pores, adhesins, phospholipases, proteases, and architectural proteins.

Autotransporters are a growing family of OMPs frequently found in pathogenic Gram-negative bacteria (7). Besides having a C-terminal transmembrane  $\beta$ -barrel domain, they also contain a soluble N-terminal domain that is displayed on the bacterial surface (8). The soluble domain is termed the passenger domain and performs the function specific for each autotransporter, whereas the transmembrane domain is termed the  $\beta$ -domain and transports the passenger domain to the external surface of the bacterium. The autotransporter secretion mechanism is unique in that all information necessary for passenger secretion is contained within one polypeptide chain; i.e., it is autotransported, a view that was challenged recently however (9). The autotransporter secretion process was first described for the *Neisseria gonorrhoeae* IgA<sub>1</sub> protease (10) but has since been identified for more

<sup>†</sup> J.E.M. and D.E.O. are supported by the Danish Technical Research Council; D.T. and M.A.S. are supported by grants from the Deutsche Forschungsgemeinschaft (DFG) (DFG SCHM 770/10-3; SFB293 B5) and the Federal Ministry for Science and Technology (BMFT) (PTJ-BIO/03U213B VBIIPG3).

\* To whom correspondence should be addressed. E-mail: dao@bio.aau.dk. Phone.: (0045) 96358525. Fax: (0045) 98141808.

<sup>‡</sup> Aalborg University.

<sup>§</sup> Westfälische Wilhelms-Universität Münster.

<sup>1</sup> Abbreviations: AIDA, adhesin involved in diffuse adherence; ANS, 8-anilino-1-naphthalenesulfonic acid; BCIP, 5-bromo-4-chloro-3-indolyl phosphate; DDM, *n*-dodecyl  $\beta$ -D-maltoside; DDPC, 1,2-didecyl-*sn*-glycero-3-phosphocholine; DHPC, 1,2-dihexanoyl-*sn*-glycero-3-phosphocholine; DLPC, 1,2-dilauroyl-*sn*-glycero-3-phosphocholine; DLS, dynamic light scattering; DM, *n*-decyl  $\beta$ -D-maltoside; DMPC, 1,2-dimyristoyl-*sn*-glycero-3-phosphocholine; DOPC, 1,2-dioleoyl-*sn*-glycero-3-phosphocholine; DPPC, 1,2-dipalmitoyl-*sn*-glycero-3-phosphocholine; DSS, disuccinimidyl suberate; lyso-DPC, 1-decyl-2-hydroxy-*sn*-glycero-3-phosphocholine; NBT, nitro blue tetrazolium; NM, *n*-nonyl  $\beta$ -D-maltoside; OG, *n*-octyl  $\beta$ -D-glucoside; OM, *n*-octyl  $\beta$ -D-maltoside; OMP, outer membrane protein; oPOE, octylpolyoxyethylene; SBTI, soybean trypsin inhibitor; SEC, size-exclusion chromatography; UM, *n*-undecyl  $\beta$ -D-maltoside.

than 120 different proteins, representing the largest group of secreted proteins in Gram-negative bacteria (11).

One of the best characterized autotransporters is AIDA from *Escherichia coli*, which due to its adhesive properties is responsible for the attachment of certain pathogenic *E. coli* strains to the intestinal lining. Thereby, the cells can colonize the gut, which under susceptible conditions might lead to diarrhea by an as yet unknown mechanism. AIDA is synthesized as a pre-pro-protein of 1286 amino acid residues (132 kDa) (12). The protein is processed N-terminally to remove the 49 amino acid signal peptide that directs the pro-protein to the periplasm. After insertion of the  $\beta$ -domain (aa's 847–1286, 47.5 kDa) into the outer membrane and translocation of the passenger domain (aa's 50–846, 79.5 kDa) to the bacterial surface, the two domains are cleaved possibly by an autocatalytic mechanism (13). After cleavage, the passenger domain remains noncovalently associated with the outer membrane. The  $\beta$ -domain consists of several domains as residues 847–949 can be removed by proteolytic cleavage of the membrane-embedded  $\beta$ -domain (1). This small surface-exposed domain, the  $\beta_1$ -domain, is predicted to form two  $\beta$ -strands on the external surface of the outer membrane. The remaining membrane-embedded core after proteolysis is termed the  $\beta_2$ -domain and consists of residues 950–1286 (36.8 kDa).

There are no high-resolution three-dimensional structures available of the different AIDA domains. The  $\beta$ -domain is located in the outer membrane and is most likely a  $\beta$ -barrel. This is supported by both bioinformatic studies and experimental data, although the exact number of  $\beta$ -strands is not known (1, 13). The recent crystal structure of the  $\beta$ -domain of NalP from *Neisseria meningitidis*, which like AIDA is classified as an autotransporter, shows a typical outer membrane  $\beta$ -barrel topology with 12 strands (9). On the basis of sequence analysis, the passenger domain of AIDA is predicted to be of the  $\beta$ -helix type, consisting of  $\beta$ -strands stacking as rungs with a triangular cross-section (14, 15) (J. E. Mogensen, unpublished results).

Biophysical characterization of OMPs in terms of folding and stability has often focused on the trimeric porins, e.g., OmpF and PhoE (16–20), and the monomeric OMPs OmpA (21–27) and OmpG (28, 29) from *Escherichia coli*. Members from other OMP families such as the ushers, secretins, autotransporters, and the Omp85 and two-partner secretion pores lack characterization despite the many members within each family (11). We have undertaken a biophysical study of the  $\beta$ -domain of AIDA to shed more light on the folding mechanism of outer membrane proteins in general and autotransporter  $\beta$ -domains in particular. In this paper, we present an analysis of the refolding properties, conformational states, and stability of the AIDA transmembrane domain, representing the first detailed biophysical characterization of an autotransporter  $\beta$ -domain.

## EXPERIMENTAL PROCEDURES

### Materials

Octylpolyoxyethylene was from Bachem AG (Bubendorf, Switzerland), 1,2-diacyl-*sn*-glycero-3-phosphocholines and 1-acyl-2-hydroxy-*sn*-glycero-3-phosphocholines were from Avanti Polar Lipids (Alabaster, AL), *n*-alkyl  $\beta$ -D-maltosides

and *n*-octyl  $\beta$ -D-glucoside were from Anatrace Inc. (Maumee, OH), Ni-NTA agarose beads were from Qiagen (Hilden, Germany), Q-Sepharose was from Pharmacia (Peapack, NJ), immobilin-P PVDF transfer membrane was from Millipore (Bedford, MA), alkaline phosphatase-conjugated AffiniPure goat anti-rabbit IgG (secondary antibody) was from Jackson ImmunoResearch Laboratories, Inc. (West Grove, PA), skim milk powder was from Fluka (Busch, Germany), NBT was from Biomol Feinchemikalien (Hamburg, Germany), BCIP was from Carl Roth (Karlsruhe, Germany), imidazole was from Acros Organics (Geel, Belgium), and SDS-PAGE low-molecular-weight markers were from MBI Fermentas (St. Leon Rot, Germany). All other chemicals were from Sigma Chemical Co. (St. Louis, MO).

### Data Analysis

Nonlinear least-squares regression analysis was carried out with Kaleidagraph, version 3.5 (Synergy Software, Reading, PA). Thermal scans were fitted to the following equation to obtain  $T_m$ , the midpoint of denaturation (30):

$$\theta = \frac{\alpha_N + \beta_N T + (\alpha_D + \beta_D T) e^{(-\Delta H_{\text{vH}}/R) \cdot (1/T) - (1/T_m)}}{1 + e^{(-\Delta H_{\text{vH}}/R) \cdot (1/T) - (1/T_m)}} \quad (1)$$

where  $\theta$  is the observed ellipticity,  $\alpha_N$  and  $\alpha_D$  are the ellipticities of the folded and denatured states, respectively, at 298 K,  $\beta_N$  and  $\beta_D$  are the slopes of the folded and denatured state baselines, respectively,  $T$  is the temperature,  $\Delta H_{\text{vH}}$  is the van't Hoff enthalpy change of unfolding, and  $R$  is the gas constant. Assuming reversible unfolding, the thermodynamic stability,  $\Delta G_{D-N}$ , at 25 °C can be calculated according to the following equation (31):

$$\Delta G_{D-N}(T) = \Delta H_{T_m} \left(1 - \frac{T}{T_m}\right) + \Delta C_p \left(-T_m + T - T \ln\left(\frac{T}{T_m}\right)\right) \quad (2)$$

where  $T_m$  is the midpoint denaturation temperature of AIDA in zero mole fraction SDS, extrapolated from a plot of  $T_m$  versus the mole fraction of SDS based on CD-monitored thermal scans (see the Results), and  $\Delta C_p$  is the specific heat capacity of unfolding.

### Construction of pDT4, pDT2, and pMS12

For the construction of pDT2 and pDT4, PCRs were performed employing the forward primers DTP1 (5'-GGGAATTCATATGCACCACCACCACCACCCTACAAAAGAAAGTGCAGG-3') and DTP3 (5'-GGGAATTCATATGCACCACCACCACCACCCTTAACCAGTCACTCTCCCACATC-3'), respectively, the reverse primer M10 (5'-GCGTAATCGATTCGCTGATAAGTTGTCCTAAGTC-3'), and pIB264 (32) as the template. The generated PCR fragments were digested with the restriction enzymes *Nde*I and *Cla*I and inserted into the vector pT7-7 (33). The resulting plasmid pDT2 codes for an N-terminal His<sub>6</sub>-tag followed by the five C-terminal amino acids of the passenger domain, and the complete  $\beta$ -domain of AIDA: MHHH-HHH-PTKES- $\beta_1$ - $\beta_2$ . pDT4 codes for the  $\beta_2$ -domain of AIDA N-terminally fused to a His<sub>6</sub>-tag: MHHHHHHH- $\beta_2$ . For the generation of pMS12 a *Sac*I/*Sma*I fragment (1.47 kb) of pMS1 (13, 34) was ligated to the vector pRSETB

(Invitrogen, Leek, NL) which was digested with *SacI* and *PvuII* prior to ligation. The resulting plasmid was designated as pMS18 (34) and digested with *ClaI* and *NdeI*. A resulting 1.53 kb fragment coding for the AIDA  $\beta$ -domain was introduced into the vector pT7-7, which was subjected to restriction with the identical enzymes prior to ligation. The generated plasmid was termed pMS12 and codes for a fusion protein consisting of an N-terminal MRGS-His<sub>6</sub>-tag, a linker region derived from the vectors pRSETB (Invitrogen, Leek, The Netherlands) and pET20 (Novagen, Madison, WI) comprising 27 amino acids, the five C-terminal residues of the passenger domain, and the complete  $\beta$ -domain of AIDA: MRGS-HHHHHH-GMASMTGGQMQGRDL-WDDDDKDPSSVD-PTKES- $\beta_1$ - $\beta_2$ .

#### Production and Purification of AIDA

**Production and Crude Purification.** Production of protein and isolation of inclusion bodies were performed essentially as described (1, 35). Briefly, *E. coli* BL21(DE3)pLysS containing pDT4 and pMS12 and *E. coli* C41(DE3) (36) containing pDT2 were grown in shaking flasks in LB medium at 37 °C and 175 rpm and induced at OD<sub>600</sub> = 0.9 with IPTG at a final concentration of 1 mM. The cultures grew for 4 h, and cells were harvested by centrifugation at 6000 rpm at 4 °C for 10 min. Cells were resuspended in 10 mL/L culture of TEN buffer (50 mM Tris, pH 8, 2 mM EDTA, 100 mM NaCl) containing 1 mM benzamidine, flash-frozen in liquid N<sub>2</sub>, and stored at -80 °C overnight. Subsequently, cells were thawed at room temperature. DNase (0.1 mg/mL) was added and the sample incubated at room temperature for 45 min. Subsequently, 1 mg/mL SBTI and 3 mM PMSF (final concentration) were added. Cells were broken by sonication (six times for 30 s at 50% intensity using a Labsonic L sonicator (Sartorius BBI Systems, Melsungen, Germany)) on ice. Inclusion bodies were collected by centrifugation at 4000g for 1 h at 4 °C and washed with 10 mL/L culture of TEN buffer containing 2% (w/w) Triton X-100 overnight at 37 °C with agitation to get rid of lipid debris. The inclusion bodies were sedimented again and washed in TEN buffer for 2 h at 37 °C with agitation to remove Triton X-100. After centrifugation, the pellet was resuspended in TN buffer (50 mM Tris, pH 8, 100 mM NaCl). Finally, this solution was centrifuged, and the pellet was stored at -20 °C until further purification.

**Purification in Detergent.** The inclusion body pellet was resuspended in 8 M urea in TN buffer (20 mL/g of pellet) and incubated for 2 h at 37 °C with agitation followed by centrifugation at 45 000g for 30 min. The supernatant, containing the solubilized protein, was mixed 1:1 with 250 mM oPOE in TN buffer and sonicated three times for 10 min at 4 °C (D-7700, Transmission Digital). Ni-NTA agarose beads were added 1:10 (v/v) to this solution and incubated for 2 h at 4 °C with agitation. This sample was loaded onto a gravity column (an empty Pharmacia PD-10 column) with a filter at the bottom allowing separation of beads and liquid. The beads were washed with 12.5 mM oPOE in TN buffer (same volume as the sample) and eluted in batch using 10  $\times$  0.5 mL of 500 mM imidazole in 12.5 mM oPOE in TN buffer. The protein was concentrated in a Centriprep YM-10 spin column (Millipore Corp., Bedford, MA) (3000g for several hours) and subsequently dialyzed against 12.5 mM oPOE in 10 mM Tris, pH 8, for 3 days at

4 °C to remove imidazole and salt for CD experiments. Typical yields of >95% pure protein were 10, 1, and 2 mg/L of cell culture for DT4, DT2, and MS12, respectively.

**Purification in Urea.** Purification of DT4 in the denatured state was performed using anion-exchange chromatography (Pharmacia Äkta Purifier system) as the Ni-NTA agarose beads gave unsatisfactory results. The inclusion body pellet was resuspended in 8 M urea in 50 mM Tris, pH 9 (20 mL/g of pellet), and incubated for 2 h at 37 °C with agitation followed by centrifugation at 45 000g for 30 min. The supernatant, containing the solubilized protein, was loaded onto an XK16 (Pharmacia, Peapack, NJ) column containing Q-Sepharose equilibrated with 50 mM Tris, pH 9. Protein was eluted using a 0–0.5 M NaCl gradient in 50 mM Tris, pH 9, and DT4 eluted at 0.3 M NaCl. The protein was concentrated in a Centriprep YM-10 spin column (3000g for several hours). The typical yield of >95% pure protein was >40 mg/L of cell culture.

**Determination of Protein Concentration.** The protein concentration was determined spectrophotometrically (UVIKON 943 Double Beam UV/vis spectrophotometer (BIO-TEK KONTRON, Milano, Italy)) at 280 nm in buffer using a molar extinction coefficient of 69130, 81220, and 85630 M<sup>-1</sup> cm<sup>-1</sup> for DT4, DT2, and MS12, respectively, as calculated from the protein sequences (37).

#### Verification of Correct Folding

**Heat-Modifiability Experiments.** Samples were mixed 5:2 with SDS-PAGE loading buffer containing 100 mM SDS and either boiled for 5 min or directly loaded onto the gel. In all experiments, 12% gels were used. Protein was detected by staining with Coomassie Brilliant Blue R-250.

**Trypsin Digestion Experiments.** Detergent- and urea-purified DT4 and detergent-purified MS12 (final concentration 1  $\mu$ M) were mixed with 28  $\mu$ g/mL trypsin in a volume of 90  $\mu$ L in 12.5 mM oPOE in TN buffer and incubated for 30 min on ice. A 10  $\mu$ L sample of CaCl<sub>2</sub> was added to a final concentration of 100 mM, and the sample was incubated at 37 °C for 30 min. Digestion was stopped by the addition of 2  $\mu$ L of SBTI to a final concentration of 0.2 mg/mL and incubation for 15 min on ice. Samples were then mixed 3:1 with SDS-PAGE loading buffer and run on a gel.

**Western Blot Procedure.** Proteins were separated on a 12% SDS-polyacrylamide gel. Transfer of proteins to a PVDF membrane was performed on a T788.1 semidry blotter (Carl Roth, Karlsruhe, Germany) at 15 V for 45 min. After transfer, the membrane was blocked in 5% (w/v) milk powder in PBS at 4 °C overnight. Antiserum raised against the AIDA  $\beta$ -domain was applied in a 1:5000 dilution in 0.5% (w/v) milk powder in PBS at room temperature. After 1 h, the membrane was washed three times for 5 min in PBS followed by incubation with a 1:5000 dilution of alkaline phosphatase-conjugated goat anti-rabbit secondary antibody in 0.5% (w/v) milk powder in PBS for 1 h at room temperature. Bound antibody was visualized after washing three times for 5 min in PBS by incubation with NBT/BCIP as the substrate in 100 mM Tris, pH 9.5, 120 mM NaCl, and 6 mM MgCl<sub>2</sub>.

#### Minimal Detergent Concentration Required To Fold AIDA DT4

Essentially, the detergent-purification procedure described above was followed. Protein in 4 M urea/125 mM oPOE in



TN buffer was mixed with beads, incubated, and loaded onto the gravity column. The beads were washed in different concentrations of oPOE in TN buffer and eluted in 500 mM imidazole in different oPOE concentrations. Samples were run on an SDS–polyacrylamide gel to test for heat modifiability.

### Conformational States of AIDA

**Fluorescence Measurements.** Steady-state fluorescence experiments were performed on an RTC2000 spectrometer from Photon Technology International (Lawrenceville, NJ). All experiments were recorded as the average of five emission scans. Excitation and emission band paths were both 5 nm. A 3 nm path length cuvette was employed. The sample was excited at 295 nm. The protein concentration was 0.5  $\mu$ M in TN buffer. All scans were recorded at 25 °C.

**Circular Dichroism Measurements.** Far-UV CD spectra were recorded on a JASCO J-715 spectropolarimeter (Jasco Spectroscopic Co. Ltd., Hachioji City, Japan) equipped with a JASCO PTC-348WI temperature control unit. The ellipticity was measured in the wavelength range of 195–245 nm, and six accumulations were averaged to yield the final spectrum. A 0.1 cm path length cuvette was employed. The protein concentration was 5  $\mu$ M in 10 mM Tris, pH 8. All scans were recorded at 25 °C.

**Acrylamide Quenching.** Urea-purified DT4 was incubated in 8 M urea, 5 mM SDS, 20 mM DM, or 8 mM DOPC in TN buffer or in TN buffer alone with 0–0.5 M acrylamide. Detergent-purified DT4 was incubated in 12.5 mM oPOE in TN buffer with 0–0.5 M acrylamide. Excitation was at 298 nm using 6 nm slit widths. Background contributions were subtracted. The emission intensity,  $F$ , at 350 nm, with background contributions subtracted, was used in the Stern–Volmer equation (38):

$$F_0/F = 1 + k_{SV}[Q] \quad (3)$$

where  $F_0$  is the fluorescence in the absence of quencher (acrylamide),  $k_{SV}$  is the Stern–Volmer constant, and  $[Q]$  is the concentration of quencher. We correct for the inner filter effect caused by the absorption of acrylamide using the equation (24)

$$F_{\text{corr}} = F \times 10^{0.275[Q]} \quad (4)$$

All experiments were performed at 20°C using 1  $\mu$ M protein.

### Size Determinations of AIDA

**Size-Exclusion Chromatography (SEC).** Gel filtration chromatography was performed on a Pharmacia LKB P-500/LCC-501 system equipped with a Superdex 200 10/30 GL column (Pharmacia, Peapack, NJ). The column was equilibrated with two column volumes of buffer (8 M urea in TN buffer, TN buffer, or 12.5 mM oPOE in TN buffer) before injection of the protein sample (100  $\mu$ L). Protein was eluted in equilibration buffer and detected by absorption at 280 nm.

**Dynamic Light Scattering (DLS).** DLS experiments were performed on a DynaPro99 molecular sizing instrument (Protein Solutions, High Wycombe, England) with a Protein Solutions temperature control unit. Samples contained 15  $\mu$ M DT4 in 8 M urea in TN buffer, TN buffer, or 12.5 mM oPOE in TN buffer and were measured at 25 °C. All samples were

filtered twice through a 100 nm filter. Dynamics version 5.25.44 was used for data acquisition and Dynals version 1.51 for data analysis using standard settings.

**Cross-Linking Experiments.** A 2  $\mu$ L sample of detergent-purified DT4 was diluted into 12.5 mM oPOE in buffer (50 mM HEPES, pH 7.4), and 2  $\mu$ L of urea-purified DT4 was diluted into 12.5 mM oPOE in buffer or buffer alone. The final protein concentration was 10  $\mu$ M. To these samples was added 1  $\mu$ L of DSS from a stock in dimethylformamide, giving a final volume of 50  $\mu$ L. The samples were incubated for 30 min at room temperature. The reaction was stopped by adding 20  $\mu$ L of SDS–PAGE loading buffer to the samples and putting them on ice before separation on 12% SDS–polyacrylamide gels.

### Characterization of the $C_w$ and $C_d$ States of DT4

**ANS Binding.** Urea-purified DT4 (5  $\mu$ M) was incubated with 5  $\mu$ M ANS for 30 min in 50 mM Tris, pH 8, or 50 mM glycine, pH 3, before measurement at 25 °C. The instrument and settings were as described above. ANS was excited at 350 nm. The contribution of buffer and protein to the measured fluorescence was subtracted.

**Thermal Denaturation.** Urea-purified DT4 (6.5  $\mu$ M) in 10 mM Tris, pH 8, was mixed with different detergents in buffer or buffer only and allowed to equilibrate for 30 min. Thermal unfolding was monitored by CD at 220 nm with a scan rate of 60 °C/h. The unfolding curves were fitted to eq 1 to obtain  $T_m$ .

### SDS-Dependent Thermal Denaturation of Refolded DT4

Thermal scans were performed on 5  $\mu$ M protein dialyzed against 12.5 mM oPOE in 10 mM Tris, pH 8. Samples were allowed to equilibrate for 30 min before measurement. Thermal unfolding was monitored by CD at 208 nm with a scan rate of 60 °C/h. Thermal unfolding curves were fitted to eq 1 to obtain  $T_m$  and  $\Delta H_{D-N}$ .

## RESULTS

**The AIDA Transmembrane Domain Can Be Expressed as Inclusion Bodies and Refolded during Purification.** The  $\beta$ -domain of AIDA is the part of the protein that remains in the outer membrane after cleavage of the passenger domain in vivo (13). We generated two constructs of AIDA encompassing the complete  $\beta$ -domain, one termed DT2 (47.8 kDa) and one termed MS12 (51.0 kDa), the latter containing 27 non-native amino acids derived from subcloning procedures. Because MS12 is expressed in higher yield than DT2 and is easier to purify, we decided to use MS12 for most experiments. Furthermore, we generated a construct encompassing the  $\beta_2$ -domain only, termed DT4 (37.6 kDa). The  $\beta_2$ -domain is the membrane-bound core left after trypsin digestion (1). None of the constructs have a signal sequence, and therefore, the proteins accumulate in the cytoplasm as inclusion bodies. A His<sub>6</sub>-tag at the N-terminus allows for Ni-affinity purification. Purification was performed in 12.5 mM oPOE using Ni–NTA agarose beads in a gravity column. Thus, the protein is refolded during purification upon transfer from urea to detergent solution. There is no functional assay for the AIDA  $\beta$ -domain to verify that the purified protein in detergent is in the native state. Instead we rely on two properties of natively folded outer membrane

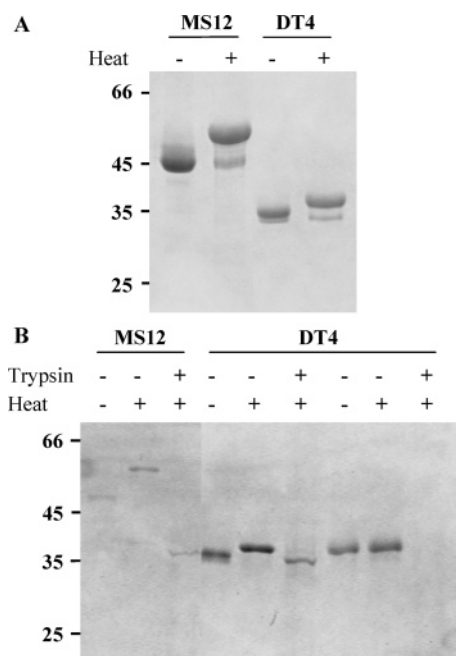


**FIGURE 1:** Verification of correct folding of AIDA DT4 and MS12. The numbers to the left on the gels represent molecular weight markers. (A) SDS-polyacrylamide gel of AIDA DT4 and MS12 purified in 12.5 mM oPOE. Both proteins display the heat shift typical of outer membrane proteins in the correctly folded state. Note that both proteins are so stable that a proportion of the protein molecules remain folded even after boiling. (B) SDS-polyacrylamide gel of trypsin-treated oPOE-purified MS12 (first three lanes), oPOE-purified DT4 (conformational state R; see Table 1) (middle three lanes), and urea-purified DT4 (conformational state C<sub>d</sub>; see Table 1) (last three lanes). All samples are in 12.5 mM oPOE in TN buffer. A core structure remains after trypsin treatment only for oPOE-purified MS12 and DT4.

proteins, namely, heat modifiability and protease protection (39, 40). DT4 and MS12 purified in oPOE both show heat modifiability (see Figure 1A), migrating faster in the nonboiled samples.<sup>2</sup> This strongly suggests that the proteins are in a nativelike conformation. Further, both proteins are resistant to proteolytic degradation as a core structure remains after incubation with trypsin (see Figure 1B). These data show that the AIDA transmembrane domain can be expressed as inclusion bodies and refolded during purification.

We used Ni-NTA agarose beads to purify DT4 in a variety of different nonionic detergents (OG, OM, NM, DM, UM, DDM), typically at 1.5–2× the cmc value. In all cases, the proteins exhibit heat modifiability (J. E. Mogensen, P. Sehgal, and D. E. Otzen, unpublished results), showing that several different detergents can promote the refolding of AIDA DT4.

*The  $\beta_2$ -Domain Requires the  $\beta_1$ -Domain or a Solid Support To Refold from the Urea-Denatured State.* We also purified DT4 in 8 M urea for subsequent refolding experiments. Urea purification was performed using anion-exchange chromatography as the Ni-affinity procedure gave unsatisfactory results (data not shown). As expected, DT4 does not exhibit heat modifiability and protease protection in 8 M urea (data

<sup>2</sup> Refolded AIDA appears as a double band on SDS-polyacrylamide gels in contrast to the denatured protein, which appears as a single band. Since the double band merges into one band upon denaturation, there are no covalent differences between the two bands of the folded protein. We do not know the origin of this phenomenon, but it has been observed previously (1).

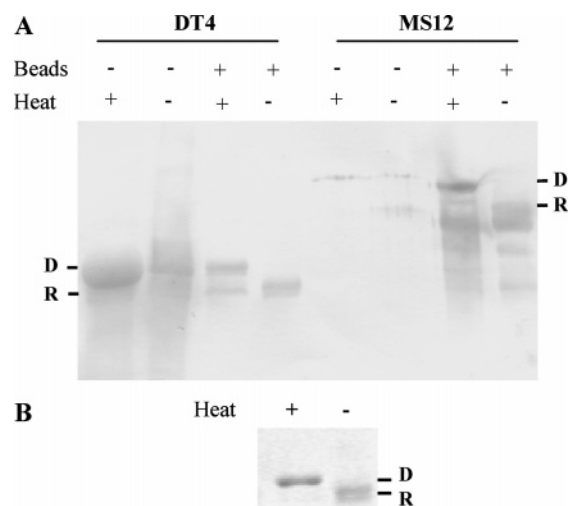


**FIGURE 2:** Refolding properties of AIDA DT4 and MS12. (A) Western blot of AIDA DT4 and MS12 before and after incubation with Ni-NTA agarose beads. Before addition of beads, the folded fraction of DT4 amounts to a maximum of 5%, while, after addition and elution, all protein is folded. For MS12, approximately 50% protein is folded before addition of beads while 100% is folded after addition and elution. The Western blot was made using primary antibodies against the  $\beta$ -domain of AIDA (see the Experimental Procedures for details). (B) SDS-polyacrylamide gel of DT4 purified in 12.5 mM oPOE using Q-Sepharose at pH 9. The protein displays heat modifiability.

not shown). We performed a comprehensive screen of the refolding capabilities of urea-unfolded DT4 by mixing the urea-purified protein with detergent micelles or phospholipid vesicles (prepared by extrusion). Several different detergents (oPOE, DDM, OG, DHPC, lyso-DPC) and phospholipids (DDPC, DLPC, DMPC, DPPC, DOPC) were tested under different conditions in terms of pH (3–10), incubation time (minutes to weeks), and temperature (4–40 °C), but we were never able to refold the protein according to the heat-modifiability and protease protection criteria (see Figure 1B). This finding raises the question as to why DT4 can refold during purification in detergent, but not when detergent is added subsequently. Purification in detergent requires the protein to bind to the Ni-NTA agarose beads, indicating that the beads might aid in folding the protein. To test this, we carried out Western blots on the DT4, DT2, and MS12 inclusion body preparations in 8 M urea mixed 1:1 with 250 mM oPOE, in the absence and presence of beads using AIDA-specific antibodies (see Figure 2A). We used Western blotting rather than Coomassie-stained gels as the AIDA inclusion body preparation contains protein contaminants since it is not yet purified. The blot shows that, in the absence of the Ni-NTA agarose beads, DT4 is not folded, while MS12 is ~50% folded, whereas after elution both proteins are 100% folded. Like MS12, DT2 also refolds with only ~50% efficiency (data not shown). DT2 and MS12, but not DT4, contain the N-terminal  $\beta_1$ -domain. Thus, the  $\beta_2$ -domain cannot fold by itself but needs the  $\beta_1$ -domain to allow at least a fraction of the protein molecules to fold. To achieve complete refolding, however, a solid support in the form of Ni-NTA agarose beads is required. The urea/oPOE AIDA samples had been incubated for several weeks at 4 °C before the Western blot analysis. Shorter incubation periods (hours to days) led to lower yields of folded MS12, indicating that the folding process under these conditions is extremely slow.

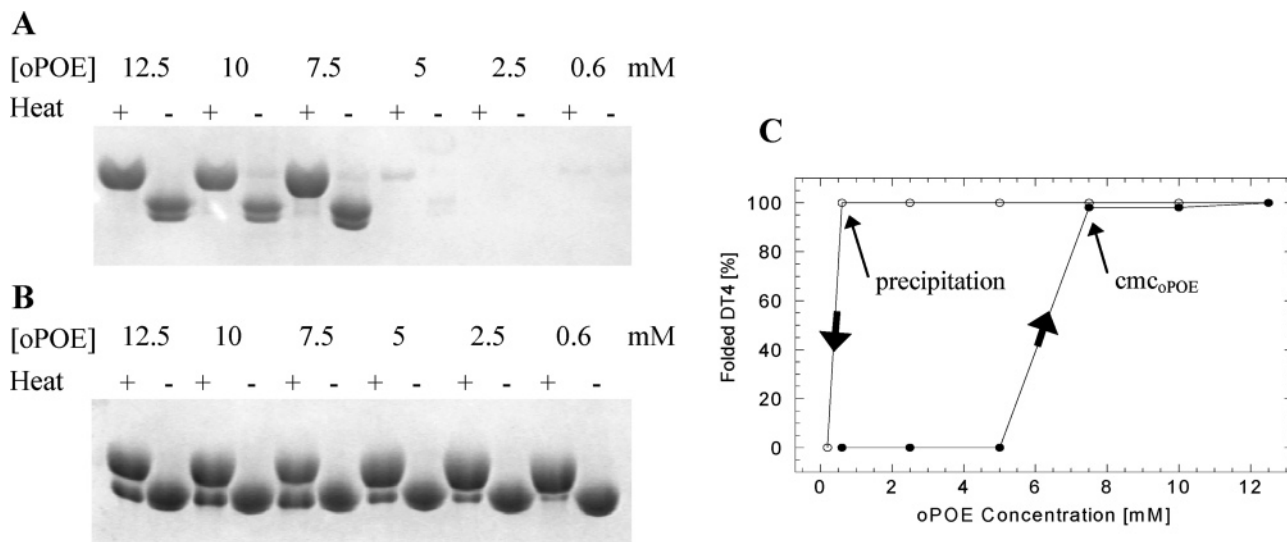


FIGURE 3: AIDA DT4 requires micellar detergent to fold but remains folded after dilution below the cmc. (A) SDS-polyacrylamide gel of DT4 eluted in various concentrations of oPOE. From 12.5 to 7.5 mM, the protein exhibits heat modifiability. From 5 down to 0.6 mM, there is no protein in the samples, indicating that it misfolds and possibly aggregates with the beads and hence does not elute. (B) SDS-polyacrylamide gel of DT4 purified in 12.5 mM oPOE and diluted to various oPOE concentrations. DT4 displays heat modifiability in oPOE concentrations 1 order of magnitude lower than the cmc (7.5 mM), revealing a kinetic barrier to the dissociation of the protein-detergent complex. (C) Schematic figure illustrating the hysteresis in the DT4 detergent dependence using the data points from the gels in (A) and (B).

To test whether a solid surface in general can support folding, we purified DT4 in oPOE using Q-Sepharose at pH 9 and tested for heat modifiability. In this case, a heat shift was apparent on the gel (see Figure 2B), demonstrating that the protein does not need to be bound to the chromatographic material only via its N-terminal His<sub>6</sub>-tail, but simply needs a solid support to refold.

**AIDA Needs Micellar Detergent To Fold.** It is a hallmark of an integral membrane protein that it needs a supramolecular assembly of amphiphiles, e.g., a micelle or a phospholipid bilayer, to fold properly. Therefore, it is expected that the folded state of AIDA can only be formed above the cmc of the detergent used (ca. 7.5 mM for oPOE under our experimental conditions), as is the case for OmpA (25). To investigate this, we purified DT4 on Ni-NTA agarose beads in different concentrations of oPOE from 0 to 12.5 mM and monitored the formation of refolded protein by heat modifiability on SDS-polyacrylamide gels. As shown in Figure 3A, the protein is properly folded from 12.5 down to 7.5 mM oPOE. Below 7.5 mM there is no protein in the samples. This probably means that the protein aggregates when eluted from the beads in detergent concentrations below the cmc, implying that the folded protein cannot form unless detergent micelles are present.

Having shown that DT4 only refolds above the cmc, we tested whether this is a reversible process by diluting the protein sample in 12.5 mM oPOE with buffer as folded membrane proteins normally precipitate when diluted below the cmc (41). It is evident from Figure 3B that DT4 remains folded even at 0.6 mM oPOE, where the detergent is present as monomers in the bulk phase. For the protein to retain its structure, detergent molecules must be bound to the protein; in other words, the oPOE molecules do not dissociate from the protein at 0.6 mM oPOE. This hysteresis-like phenomenon (see Figure 3C) implies that there is a kinetic barrier to the dissociation of the protein-detergent complex. The possibility that the detergent can form clusters on the protein

surface below its bulk cmc is ruled out by the purification experiments at different oPOE concentrations, where super-cmc concentrations are required for refolding. Note from Figure 3B that, below the cmc, the fraction of folded protein decreases with decreasing oPOE concentration, implying that the protein is destabilized when bulk micelles are no longer present. If DT4 is diluted to 0.2 mM oPOE, it precipitates, showing that the minimal oPOE concentration required to keep the folded protein in solution is between 0.6 and 0.2 mM.

**Conformational States of the AIDA  $\beta$ -Domain.** We investigated the conformational properties of AIDA DT4 under different solution conditions using tryptophan fluorescence, CD spectroscopy, and protease digestion experiments. The result of secondary structure predictions based on far-UV CD scans as well as a summary of the properties of the different conformational states of DT4 are listed in Table 1.

DT4 purified in oPOE displays a fluorescence emission spectrum with high intensity and an emission maximum of 335 nm, indicating that the tryptophans reside in a hydrophobic environment (see Figure 4A). Its far-UV CD spectrum shows a typical  $\beta$ -structure profile with the characteristic minimum at 215 nm and a zero-ellipticity crossover at approximately 207 nm (see Figure 4B). Together with heat modifiability and trypsin protection, as described in the previous section, these are typical features of a natively like outer membrane protein (42). We term this state the refolded or R state.

DT4 purified in 8 M urea shows an emission spectrum with low intensity and an emission maximum of 348 nm, indicating that the tryptophans are in a polar environment with high solvent accessibility (Figure 4A). Consistent with this, the far-UV CD spectrum is indicative of a random-coil-like conformation (Figure 4B). We term this state the denatured or D state.

In contrast to inner membrane proteins, it is not unusual for outer membrane proteins to remain soluble in the absence



Table 1: Properties of Conformational States Formed by AIDA DT4

	D	C <sub>w</sub>	C <sub>d</sub>	R
water solubility	yes	yes	yes	no
heat modifiability	no	no	no	yes
protease protection	no	no	no	yes
aggregation state	monomeric	oligomeric	oligomeric	monomeric
T <sub>m</sub> (°C)		~70	~73	~113
ΔG <sub>D-N</sub> (kcal/mol)		~3 <sup>b</sup>	~3–4 <sup>b</sup>	~12
secondary structure <sup>a</sup>	random coil	α (10%) β (31%) random coil/turns (60%)	α (13%) β (27%) random coil/turns (60%)	α (6%) β (45%) random coil/turns (48%)

<sup>a</sup> Secondary structure content predicted using available programs on DICHROWEB (71). The percentages are the average of seven outputs using Selcon3 (reference sets 4 and 7), CONTIN (reference sets 4 and 7), CDSSTR (reference sets 4 and 7), and K2D. <sup>b</sup> Determined from urea denaturation experiments (J. E. Mogensen and D. E. Otzen, unpublished observations).

of detergent (16, 29) because they do not contain long contiguous segments of hydrophobic amino acids (43). In accordance with this, we found that urea-purified DT4 at low micromolar concentrations can be diluted into buffer without any precipitation occurring. The tryptophan emission displays a large blue shift to 335 nm concomitant with an increase in intensity, indicating a hydrophobic environment of the tryptophans (Figure 4A). The far-UV CD spectrum displays a minimum at 215 nm, indicating a significant amount of  $\beta$ -structure; however, the zero-ellipticity crossover is at 200 nm, suggesting that the structure is non-native (Figure 4B). Also, the protein does not show heat modifiability on SDS–polyacrylamide gels and is sensitive to proteolysis (data not shown). These data indicate that, upon dilution of the denaturant, DT4 adopts a partially folded state (designated C<sub>w</sub>) which is rich in  $\beta$ -sheet structure but non-native, as might be expected in the absence of detergent.

If the urea-purified protein is diluted into detergent solution, the fluorescence and CD spectra do not coincide with the ones obtained for the refolded state in agreement with the finding that refolding in the absence of a solid support does not produce heat-modifiable protein. Instead, the spectra more resemble those of the C<sub>w</sub> state although with higher fluorescence intensity and a slightly higher ellipticity at 215 nm (Figure 4A,B). This suggests that the protein is not structured to the same extent as when detergent was present during purification, and therefore, it represents a misfolded state (designated C<sub>d</sub>).

To extend the structural analysis, we probed the environment of the tryptophan residues under different solution conditions using acrylamide quenching of tryptophan fluorescence (see Figure 4C). This is a measure of the accessibility of the tryptophan side chains to a polar but uncharged molecule. The fitted Stern–Volmer constants are shown in Table 2. The more solvent-accessible the tryptophan side chains are, the higher the Stern–Volmer constants will be (38). In the urea-denatured state, the tryptophans display the highest solvent accessibility. In C<sub>w</sub>, the tryptophans are less accessible, and in C<sub>d</sub> even more so. For the refolded protein, the tryptophans are slightly less buried compared to those in C<sub>d</sub>. Thus, the quenching experiments are in agreement with the fluorescence spectra in Figure 4A.

*Gel Filtration and DLS Experiments Show the Refolded State Is Monomeric and the C States are Oligomeric.* To determine the size of the different conformational states of AIDA DT4, we used SEC, DLS, and DSS cross-linking experiments. Detergent-purified DT4 in 12.5 mM oPOE gave

a single elution peak in SEC, corresponding to a mass of approximately 79 kDa as calculated from a protein calibration curve in 12.5 mM oPOE (data not shown). Using DLS, the hydrodynamic radius measured from several independent experiments was  $4.17 \pm 1.10$  nm. As a control we measured the size of the oPOE micelles in the absence of protein. This gave a hydrodynamic radius of  $2.7 \pm 0.5$ , showing that the micelle size changes to accommodate the protein molecules. Using a standard protein molecular weight model, the size of DT4 corresponds to a molecular weight of approximately 92 kDa, in reasonable agreement with the gel filtration experiment. The theoretical mass of DT4 from the protein sequence is 37.6 kDa, implying that 41.4–54.4 kDa of detergent is associated with the protein. The average molecular mass of oPOE is 400 Da, implying that approximately 100–140 detergent molecules are associated with one folded monomer of DT4. In principle, a mass of 79–92 kDa is consistent with a dimer; however, this would only leave 3.8–16.8 kDa of detergent to be associated with two protein molecules, which we consider unlikely as the protein is nativelike and therefore most likely surrounded by a large coat of detergent molecules (44). In addition, the SDS–PAGE migratory behavior of the folded state suggests a monomeric protein, although dissociation of a putative dimer in SDS cannot be ruled out.

In SEC, urea-purified DT4 in 8 M urea elutes with a single peak corresponding to a mass of approximately 79 kDa as calculated from a protein calibration curve in 8 M urea (data not shown). A priori, this could be interpreted as a dimer; however, under these conditions the protein is completely denatured. Thus, the lack of associated detergents compared to the refolded state in oPOE is probably compensated by the increased hydrodynamic radius of the polypeptide chain.

Urea-purified DT4 diluted into buffer (C<sub>w</sub>) displays a heterogeneous elution profile in SEC with two elution peaks corresponding to a mass of ~170 and ~400 kDa as calculated from a protein calibration curve in buffer (data not shown). This indicates that, in the absence of detergent, the protein forms heterogeneous aggregates of ~4–10 monomers.

Urea-purified DT4 in 12.5 mM oPOE (C<sub>d</sub>) yields a hydrodynamic radius of 10–17 nm in DLS experiments (data not shown). This implies that also in the presence of detergent the urea-purified protein forms large heterogeneous aggregates; however, these are significantly larger than for C<sub>w</sub>.

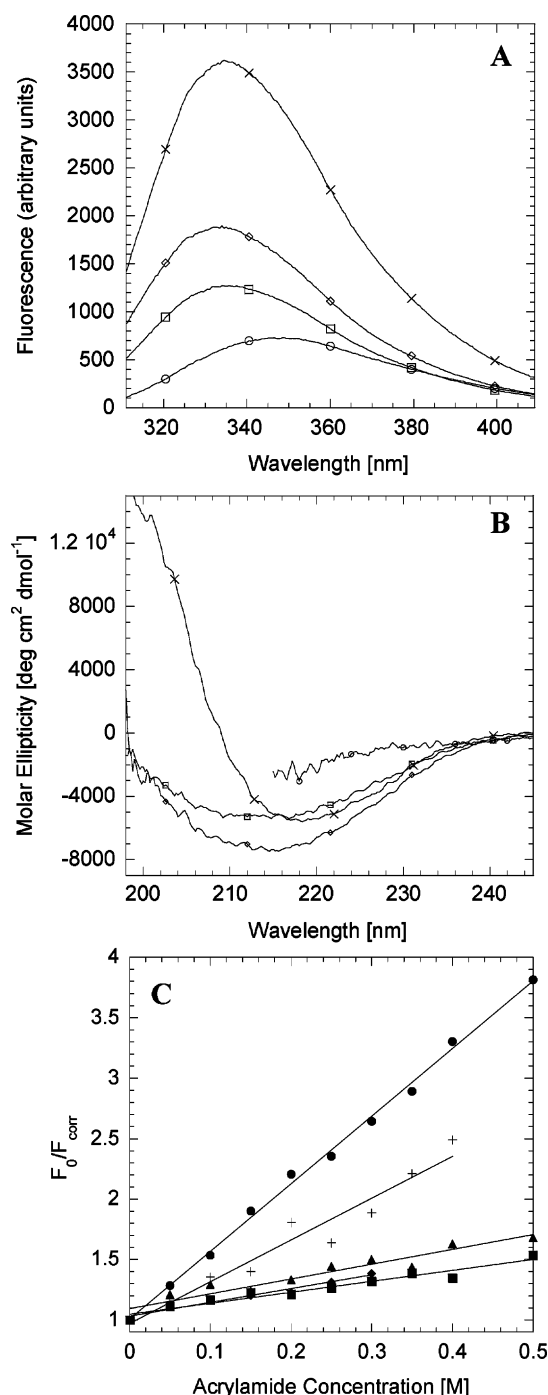


FIGURE 4: Conformational states of AIDA DT4. (A) Fluorescence emission spectra of (○) urea-purified DT4 in 8 M urea, (□) in buffer, and (◇) in 12.5 mM oPOE and (×) detergent-purified DT4 in 12.5 mM oPOE. All solutions were in TN buffer, and experiments were performed at 25 °C using 0.5  $\mu$ M protein. (B) Far-UV CD spectra of (○) urea-purified DT4 in 8 M urea, (□) in buffer, and (◇) in 12.5 mM oPOE and (×) detergent-purified DT4 in 12.5 mM oPOE. All solutions were in 10 mM Tris, pH 8, and experiments were performed at 25 °C using 5  $\mu$ M protein. (C) Stern–Volmer plots of (●) urea-purified DT4 in 8 M urea, (+) in buffer, (◆) in 8 mM DOPC, and (■) in 20 mM DM and (▲) detergent-purified DT4 in 12.5 mM oPOE. The solid lines represent the best fit to eq 3. All solutions were in TN buffer, and experiments were performed at 20 °C using 1  $\mu$ M protein.

Finally, we performed cross-linking experiments with DSS, a homobifunctional cross-linking reagent with amine reactivity that incorporates an eight-atom linker. These experiments showed  $C_w$  and  $C_d$  to be oligomeric and R to be monomeric

on SDS–polyacrylamide gels in agreement with the results of the SEC and DLS experiments (data not shown).

In conclusion, refolded DT4 behaves as a monomer in detergent solution, while the water-soluble form and the misfolded form in detergent are present predominantly as large aggregates.

*C<sub>w</sub> and C<sub>d</sub> Are Not “Molten-Globule-like” at Neutral pH, Unfold Cooperatively, and Cannot Be Converted to R.* As mentioned, urea-purified DT4 remains soluble in buffer in the absence of denaturant or detergent. We tested whether the water-soluble state is molten-globule-like using the fluorescent probe ANS, which has affinity for such partially folded states (45). At neutral pH (pH 8), no increase in ANS fluorescence was detected upon addition of  $C_w$  to ANS in buffer (data not shown). However, at acidic pH (pH 3), a large increase in ANS fluorescence is evident in the presence of  $C_w$ , indicating binding of the probe to the protein (data not shown).

We probed the cooperativity of the  $C_w$  state at neutral pH (pH 8) by CD-monitored thermal scans. The unfolding curve displays a sharp transition with a midpoint of unfolding,  $T_m$ , of  $70.2 \pm 0.0$  °C, showing that the  $C_w$  state is a cooperative structure with significant tertiary interactions (see Figure 5). Addition of detergent at 1.5–2 $\times$  the cmc to  $C_w$ , leading to the formation of  $C_d$ , did not significantly affect  $T_m$  (see Figure 5). These data show that even a misfolded state of the AIDA  $\beta$ -domain is quite stable. For comparison, the water-soluble state of OmpG displays a  $T_m$  of  $34.1 \pm 0.6$  °C (29).

Finally, we incubated  $C_w$  with Ni–NTA agarose beads under refolding conditions to test whether the water-soluble state could be converted to R. This was not the case as no heat modifiability was observed on SDS–polyacrylamide gels (data not shown), and therefore,  $C_w$  appears to be genuinely misfolded.

*The AIDA  $\beta$ -Domain Is Extremely Thermostable.* We measured the thermal stability of refolded DT4 and MS12 by CD spectroscopy. Thermal scans at 215 nm in different detergents at 1.5–2 $\times$  the cmc showed no transition up to 100 °C, indicating extreme thermal stability of the  $\beta$ -domain (data not shown). Therefore, we included SDS in the samples to lower  $T_m$  to an experimentally accessible temperature. The presence of SDS does not change the structure of the protein as judged from far-UV CD scans (see Figure 6A) but merely destabilizes it. Thermal denaturation in a mixed oPOE/SDS system was monitored by far-UV CD at 208 nm because SDS induces  $\alpha$ -helical structure upon denaturation (46), leading to a large change in the CD signal at this wavelength (see Figure 6A). Heating DT4 gives rise to a sharp transition whose midpoint is dependent on the amount of SDS present in the system (see Figure 6B).  $T_m$  shows pronounced curvature versus absolute SDS concentration (see the inset of Figure 6C); however, when plotted against the bulk SDS mole fraction, there is a reasonably linear correlation (Figure 6C). Extrapolation to zero mole fraction SDS suggests a melting temperature of around  $112.9 \pm 1.2$  °C in pure oPOE micelles, making the transmembrane domain of AIDA an extremely thermostable protein. Using this method, we can determine the thermal stability in different detergents. The extrapolated  $T_m$  values vary significantly with detergent headgroup and chain length (J. E. Mogensen, P. Sehgal, and D. E. Otzen, unpublished results). The thermal denaturation process is completely irreversible as the far-UV CD



Table 2: Stern–Volmer Constants As Determined from Acrylamide Quenching of Tryptophan Fluorescence for the Different Conformational States of AIDA DT4<sup>a</sup>

DT4 conformational state	condition	$k_{SV}$ (M <sup>-1</sup> )	DT4 conformational state	condition	$k_{SV}$ (M <sup>-1</sup> )
R	12.5 mM oPOE	1.22 ± 0.13	C <sub>w</sub>	buffer	3.45 ± 0.32
C <sub>d</sub>	20 mM DM	0.91 ± 0.08	D	8 M urea	5.59 ± 0.11
C <sub>d</sub>	8 mM DOPC	1.14 ± 0.10			

<sup>a</sup> Experiments are performed at 20 °C in TN buffer. The error stated is the error of the fit.

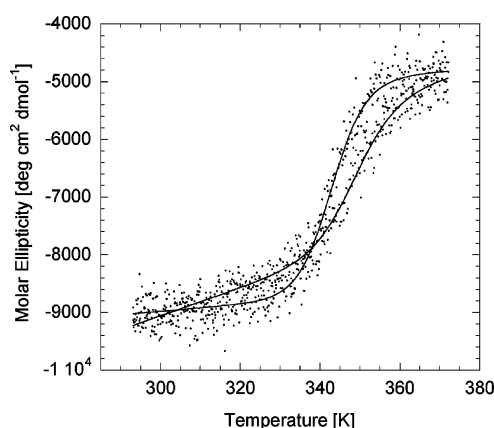


FIGURE 5: The C<sub>w</sub> and C<sub>d</sub> states of DT4 unfold cooperatively. Thermal scans of 10 μM urea-purified DT4 in 10 mM Tris, pH 8 (curve with left-most transition) and in 25 mM oPOE in 10 mM Tris, pH 8 (curve with right-most transition), as monitored by far-UV CD at 220 nm. The solid lines represent the best fit to eq 1 yielding a  $T_m$  value of 70.2 ± 0.0 and 73.0 ± 1.0 °C, respectively.

spectrum of the cooled sample shows that the protein is  $\alpha$ -helical in structure (see Figure 6A). This means that a kinetic trap prevents the protein from refolding from the non-native  $\alpha$ -helical state to the refolded  $\beta$ -barrel state.

Since earlier studies indicated that the  $\beta_1$ -domain increases the stability of the  $\beta_2$ -domain (1), we investigated the stability of the MS12 protein by the same method (see Figure 6C). Extrapolation of  $T_m$  to zero mole fraction SDS suggests a melting temperature of around 132.7 ± 12.2 °C in pure oPOE, which is ~20 °C higher compared to that of the DT4 protein. Thus, the  $\beta_1$ -domain increases the thermal stability of the  $\beta_2$ -domain significantly.

For reversibly unfolding proteins,  $T_m$  is merely the ratio between its enthalpy and entropy of unfolding (47). We therefore sought to determine the stability of AIDA in terms of its free energy of unfolding,  $\Delta G_{D-N}$ , which can be calculated if the heat capacity of unfolding,  $\Delta C_p$ , is known. Since DT4 does not unfold reversibly, our conclusion should only be seen as a general indication of the protein's stability level. The model used to fit the thermal scans of DT4 in oPOE/SDS provides us with the enthalpy of unfolding,  $\Delta H_{D-N}$  (see eq 1). It was not possible to determine a  $\Delta C_p$  value for MS12 due to large scatter in the  $\Delta H_{D-N}-T_m$  plot (data not shown). However, for DT4 we find a reasonably linear relationship between  $\Delta H_{D-N}$  and  $T_m$  (see Figure 6D). The slope of the fitted curve is  $\Delta C_p$ , which yields 820 ± 154 cal/(mol K). This translates into a  $\Delta G_{D-N}$  value of approximately 12 kcal/mol using eq 2. The determined stability lies within the normal range found for water-soluble proteins (5–15 kcal/mol, 48). However, the denatured state in our system is significantly structured (due to the presence of SDS). Therefore, the calculated stability does not represent

the difference in free energy between the unfolded and folded states ( $\Delta G_{D-N}$ ) but rather between a misfolded state and the folded state. This may underestimate the “true” thermodynamic stability.

## DISCUSSION

**Refolding Properties of the AIDA  $\beta$ -Domain.** Studies have shown that the  $\beta_2$ -domain of AIDA can be natively integrated into the outer membrane *in vivo* without the presence of the  $\beta_1$ -domain or the passenger domain provided it is preceded by the signal sequence in the expression vector (13, 49). Thus, in principle, the  $\beta_2$ -domain constitutes a coherent folding unit by itself although it is not known if the refolding rate or yield is affected in the absence of the  $\beta_1$ -domain. Despite this, we find that, *in vitro*, the  $\beta_2$ -domain is unable to refold. Complete refolding, however, can be achieved in the presence of a solid support in the form of chromatographic material. When the  $\beta_1$ -domain is present, folding occurs to about 50% efficiency without a solid support, although this reaction is extremely slow. In principle, we cannot discount that the fact that AIDA cannot refold in solution is an *in vitro* artifact. We strongly believe this is not the case as we performed an extensive screening of refolding conditions. Also, we did not test specifically whether the His<sub>6</sub>-tag interferes with folding. However, we consider interference very unlikely as DT4, DT2, and MS12 are able to fold with 100% refolding yields on both the Ni-NTA agarose and the Q-Sepharose beads. Furthermore, the protein DT1, which also contains an N-terminal His<sub>6</sub>-tag and is similar to DT2 but in addition contains the native AIDA signal sequence, can become natively integrated into the outer membrane *in vivo* (50). Thus, we believe that the behaviors of DT4, DT2, and MS12 are no different from those of their His<sub>6</sub>-tag-free counterparts.

There are many examples of OMPs that can be fully reconstituted *in vitro* simply by dilution of the urea-unfolded protein into micelles or vesicles either directly or via dialysis (51). This is also the case for autotransporter  $\beta$ -domains (9, 52). There are exceptions, however. The Toc75 protein from the outer membrane of chloroplasts shows behavior similar to that of AIDA as it can only fold *in vitro* using Ni-chelate chromatography (53). Furthermore, OmpF, a trimeric porin, and FhuA, a siderophore receptor, both from *E. coli*, display low folding yields *in vitro*, OmpF only folding with ca. 30% efficiency in lipid bilayers at optimal conditions (16, 54). This has been ascribed to fast aggregation of the OMPs, which competes with bilayer insertion and folding (54). Also, in the case of OmpA, aggregation competes with folding. At neutral pH, the folding efficiency is only 70% although it approaches 100% at pH 10 (22). Porin from *Rhodospseudomonas blautica* and OMPLA from *E. coli* also display low refolding yields *in vitro* (35, 55).

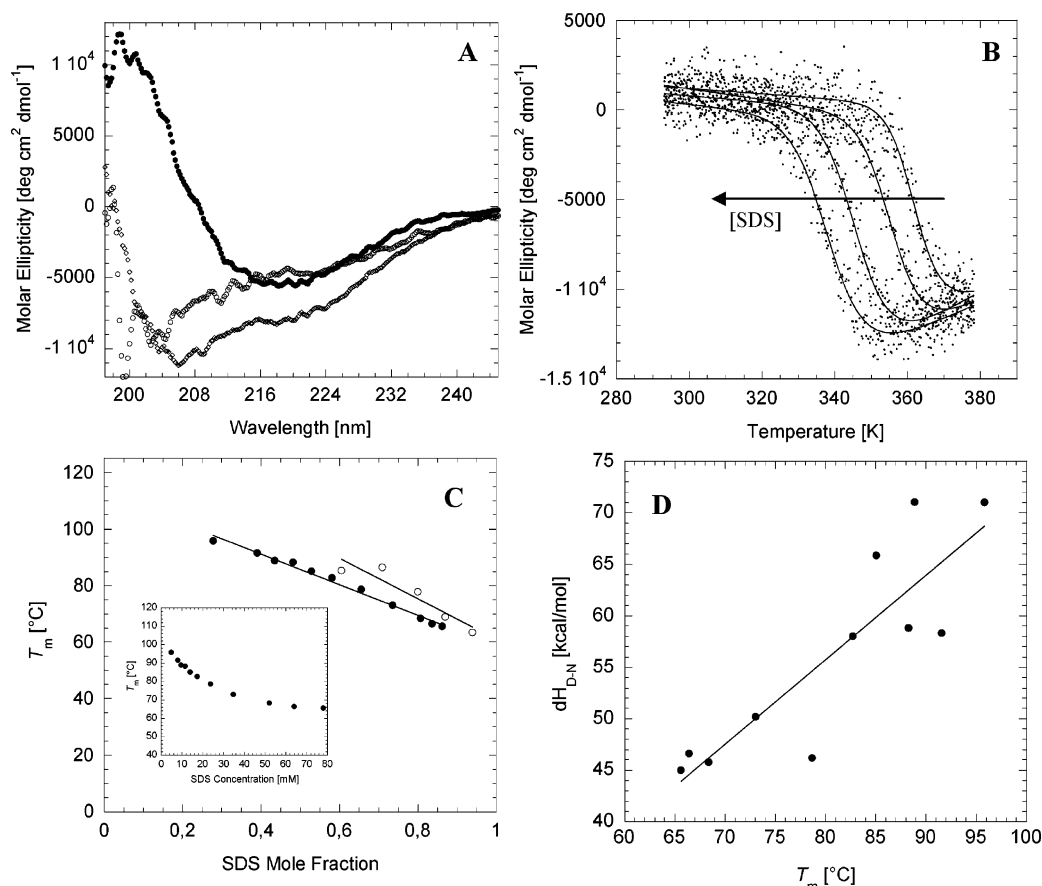


FIGURE 6: Stability of refolded AIDA. (A) Far-UV CD scans of 5  $\mu$ M detergent-purified DT4 in 12.5 mM oPOE and 50 mM SDS in 10 mM Tris, pH 8, showing that the refolded state is maintained in the presence of SDS (●). At 105  $^{\circ}$ C the protein is denatured but not unfolded as SDS induces  $\alpha$ -helical structure in the denatured state (○). After cooling to 25  $^{\circ}$ C, the  $\alpha$ -helical structure is retained as unfolding is irreversible also in the presence of SDS (◇). (B) Representative far-UV CD thermal scans of oPOE-purified DT4 in various SDS concentrations ([oPOE] = 12.5 mM, and [SDS] = 9.6, 17.4, 34.7, or 78 mM). Increasing concentrations of SDS shift  $T_m$  to lower values. The solid lines represent the best fit to eq 1. Same conditions as in (A). (C) Thermal stability of oPOE-purified DT4 and MS12. When  $T_m$  versus SDS mole fraction is plotted, a reasonably linear relationship is observed. The solid lines represent the best linear fits to the data whereby  $T_m$  in 12.5 mM oPOE alone can be estimated to be  $112.9 \pm 1.2$  and  $132.7 \pm 12.2$   $^{\circ}$ C for DT4 and MS12, respectively. Inset:  $T_m$  of DT4 as a function of the absolute SDS concentration yields significant curvature. (D) Enthalpy of unfolding,  $\Delta H_{D-N}$ , versus  $T_m$  for DT4. The enthalpies are derived from eq 1. The solid line represents the best linear fit to the data, yielding a slope of  $820 \pm 154$  cal/(mol K), which is the heat capacity of unfolding,  $\Delta C_p$ .

The AIDA  $\beta$ -domain is prone to aggregation as it forms oligomeric complexes when diluted from 8 M urea into buffer or detergent solution. These higher order structures apparently represent a dead-end state from which productive folding cannot proceed although micelles are present upon dilution of the denaturant, and thus should shield against unwanted intermolecular contacts. Apparently, intramolecular collapse of the unfolded polypeptide chains occurs so quickly that proper folding cannot occur. AIDA (average hydrophobicity 0.28)<sup>3</sup> does not contain more hydrophobic residues when compared to the  $\beta$ -barrel domains of OmpG (0.28), OmpA (0.28), OmpX (0.26), and FhuA (0.31), which are also monomeric. Thus, the inability to refold in solution cannot in principle be ascribed to a higher propensity of AIDA to aggregate if one assumes that increased hydrophobicity leads to higher aggregation tendency. The fact that the  $\beta_1$ -domain aids in refolding does, however, suggest that solubility might be a key issue as this domain is predicted

not to be intramembranous and, therefore, would increase the solubility of the protein.

Taken together, there are two ways in which AIDA can be refolded without being trapped in a misfolded state: using either a solid support or an extension of the protein to include the  $\beta_1$ -domain. Both remedies introduce the possibility of avoiding inappropriate interactions, in one case by anchoring the protein to a surface and in the other case by introducing extra residues which may engage the rest of the protein in specific contacts. This is analogous to the concept of gatekeeper residues, which we recently proposed as a class of residues which prevent undesirable interactions (such as those stabilizing misfolded or aggregated states), rather than directly stabilizing the native state (56–59). It is remarkable that for AIDA DT4 no detectable fraction of the protein population refolds in solution, whereas 100% refolding occurs on the beads. This further indicates that the role of the solid support is to prevent the formation of unproductive misfolded conformations possibly by effectively lowering the protein crowding effect and allowing folding independently of other unfolded protein molecules.

<sup>3</sup> The number denotes the number of hydrophobic residues alanine, valine, leucine, isoleucine, phenylalanine, and methionine relative to the total number of residues in the sequence.

**Functional Significance of the  $\beta_1$ -Domain.** Chaperoning by certain regions of autotransporter proteins has been described earlier. In the *Serratia marcescens* autotransporter protease PrtS, a region termed the junction region, was found to be essential for proper folding of the passenger domain (60). This junction region remains associated with the  $\beta$ -domain after cleavage of the passenger domain. Very recently, Oliver et al. identified a region of the BrkA autotransporter, which is necessary for proper folding of the passenger domain on the bacterial surface (15). In this case, contrasting with PrtS, the junction region remains associated with the passenger domain after proteolytic processing. Sequence analysis showed this conserved domain, termed PD002475, to be present in more than 55 autotransporter proteins including AIDA (15). In AIDA, the PD002475 domain corresponds to the  $\beta_1$ -domain. Consequently, the function of PD002475 may not only be to aid in the folding of the passenger domain but also to chaperone the  $\beta_2$ -domain. For BrkA and PrtS, the junction region could be complemented in trans in vivo. We are currently investigating whether this is the case for AIDA in vitro.

Besides chaperoning the  $\beta_2$ -domain, we also found a stabilizing effect of the  $\beta_1$ -domain as was reportedly earlier (1). This raises the question as to whether the stability increase of the  $\beta$ -domain due to the  $\beta_1$ -domain has any functional significance. After proteolytic cleavage in vivo, the passenger domain of AIDA remains bound to the bacterial surface (13), presumably by binding to the  $\beta$ -domain. Continued association of the passenger domain with the bacteria is probably vital for virulence. In this respect, the stability, and thereby the integrity, of the  $\beta$ -domain becomes important not only for secretion of the passenger domain across the outer membrane but also for the ability of the bacterium to colonize its host.

**Detergent-Purified AIDA Is Nativelike, Not Water-Soluble, and Extremely Thermostable.** During purification upon transfer from urea to detergent solution, the  $\beta$ -domain of AIDA can be refolded. The purified protein displays the classical characteristics of a natively folded outer membrane protein, namely, heat modifiability on SDS–polyacrylamide gels and resistance to degradation by trypsin.

In contrast to  $C_w$ , R is not water-soluble as it precipitates below 0.6 mM oPOE. This can probably be ascribed to the fact that, in the folded conformation, the polarity of the barrel is established with a hydrophobic face on the outer surface and a hydrophilic face inside the barrel (cf. the NaIP structure). Below a certain detergent concentration threshold, too few detergent monomers remain bound to the barrel to prevent the protein molecules from associating via their hydrophobic faces. In contrast, this structural polarity is not established when the protein is transferred to water from the denatured state in urea, leading to a lower precipitation propensity although it still oligomerizes.

In the recently determined crystal structure of the NaIP  $\beta$ -domain, an  $\alpha$ -helix was found in the lumen of the barrel (9). Residues ca. 951–1002 of AIDA are also predicted to form an  $\alpha$ -helix (9, 15). The secondary structure prediction estimates ca. 6%  $\alpha$ -helix in DT4 in oPOE (see Table 1), which corresponds to 20–21 residues adopting an  $\alpha$ -helical conformation. This should be sufficient to traverse a  $\beta$ -barrel structure given that one residue contributes 1.5 Å in an  $\alpha$ -helix (61) and that the thickness of the hydrocarbon part

of a bilayer and thereby a minimal  $\beta$ -barrel is approximately 30 Å (62). It is therefore possible that an  $\alpha$ -helix is formed in the lumen of the DT4 barrel in the detergent-folded protein.

On the basis of CD-monitored thermal scans of DT4, we estimate a  $T_m$  value of  $112.9 \pm 1.2$  °C in 12.5 mM oPOE, making DT4 an exceptionally heat-stable protein. Outer membrane proteins are generally very heat-stable, and have a remarkable resistance to SDS, which is also the basis for the observed heat modifiability these proteins display on SDS–polyacrylamide gels when correctly folded. Another remarkably heat-stable outer membrane protein is LamB from *E. coli*, which resists boiling for at least 60 min in a mixture of Triton X-100 and SDS; however, LamB contains a disulfide bridge that augments its stability, a feature that is very rare in the transmembrane domains of OMPs (63). Also, the octameric porin MspA from *Mycobacterium smegmatis* is extremely heat-stable, having a  $T_m$  of 112 °C in 12.5 mM oPOE (64). Thermal stabilities of FhuA and OmpF have also been reported in micellar systems. OmpF in a mixture of oPOE and SDS (it is not clear at which mole fraction) displays a  $T_m$  of 72 °C (65). FhuA in 0.03% *N,N*-dimethyldodecylamine *N*-oxide (LDAO) shows  $T_m$  values of 65 and 75 °C for the cork and the barrel domains, respectively, whereas deletion of the cork domain reduces  $T_m$  to ~62 °C (66). Thus, the soluble domain that resides in the barrel cavity stabilizes the barrel structure. For AIDA, it is possible that the proposed  $\alpha$ -helix residing in the lumen of the barrel also stabilizes the protein. It would be interesting to determine the stability of the barrel in the absence of the linker region.

On the basis of the thermal stability and predicted heat capacity of unfolding, we estimate an apparent thermodynamic stability of ~12 kcal/mol for AIDA DT4. Very recently, a reversible system was established for OmpA, allowing true thermodynamic parameters to be determined. OmpA was reconstituted in small unilamellar vesicles and denatured by urea. Here, [urea<sup>50%</sup>] values of ca. 3 M were observed with an associated  $m$  value of ca. 1 kcal/(mol M), resulting in free energies of ca. 4 kcal/mol in a reference POPC/POPG system, which is predicted to increase to ca. 7 kcal/mol by the addition of POPE (67). This is significantly lower than what we find for AIDA especially when it is considered that AIDA was studied in a micellar system and OmpA in a vesicle system as OMPs are generally more stable in a bilayer than in detergent micelles. The low stability of OmpA may be linked to the high pH (10.0) used in the unfolding experiments, a condition which probably is necessary to ensure full reversibility. The misfolded state of AIDA  $C_d$  displays a free energy of unfolding (ca. 3 kcal/mol) (see Table 1) comparable in magnitude to that of folded OmpA, and there is no doubt that the R state of AIDA is significantly more stable. We also tried urea unfolding folded DT4 in 12.5 mM oPOE, but observed no changes in secondary structure even at 6 M urea (data not shown).

**Barriers to Folding and Unfolding.** AIDA is characterized by kinetic barriers in both folding and unfolding. First, although the  $\beta_2$ -domain in vivo can become natively integrated into the outer membrane of *E. coli* (13, 49), in solution it cannot refold, but requires either the  $\beta_1$ -domain or a solid support. Second, it displays clear hysteresis in its detergent dependence, since it shows an absolute requirement



for micellar oPOE for folding on Ni-NTA agarose beads, but can tolerate much lower detergent concentrations once it is folded. This is corroborated by its thermal stability; the protein cannot refold from the urea-denatured state on a solid support in SDS, yet thermal scans at different SDS mole fractions predict that the  $T_m$  in 100% SDS is around 60 °C. Thus, there is a strong barrier to the dissociation of the oPOE molecules, maintaining the protein in the folded conformation.

Previous work on the folding of other bacterial outer membrane proteins such as OmpA and OmpF shows that folding is a remarkably slow process (16, 22, 23, 54), revealing significant activation barriers to the process. This is no doubt related to the highly cooperative nature of folding of  $\beta$ -barrel proteins, where individual segments are unlikely to fold on their own because of the requirement of extensive hydrogen bonding between the different  $\beta$ -strands. This is also seen for water-soluble proteins of the  $\beta$ -barrel type, which often have a transition state for folding (expressed by the  $\beta_T$  value) that is very close to the native state on the reaction coordinate, implying extensive cooperativity. This is exemplified by CspB, consisting of two small  $\beta$ -sheets forming a closed barrel structure, which has a  $\beta_T$  value of  $\geq 0.9$  (68). In contrast, folding of an  $\alpha$ -helical protein, such as DsbB, in detergents from the SDS-denatured state occurs in a matter of seconds (69), probably because the  $\alpha$ -helices can fold very rapidly on their own and subsequently dock against each other to form the native structure, as suggested by the two-state model of helical membrane protein folding (70).

## ACKNOWLEDGMENT

We thank Daniel Müller for developing the detergent-based purification procedure and Jeppe B. Jensen for helping with the gel filtration experiments.

## REFERENCES

- Konieczny, M. P. J., Benz, I., Hollinderbäumer, B., Beinke, C., Niederweis, M., and Schmidt, M. A. (2001) Modular organization of the AIDA autotransporter translocator: The N-terminal  $\beta_1$ -domain is surface-exposed and stabilizes the transmembrane  $\beta_2$ -domain, *Antonie van Leeuwenhoek* 80, 19–34.
- Wimley, W. C. (2003) The versatile  $\beta$ -barrel membrane protein, *Curr. Opin. Struct. Biol.* 13, 404–411.
- Faller, M., Niederweis, M., and Schulz, G. E. (2004) The Structure of a Mycobacterial Outer-Membrane Channel, *Science* 303, 1189–1192.
- Wimley, W. C. (2002) Toward genomic identification of  $\beta$ -barrel membrane proteins: Composition and architecture of known structures, *Protein Sci.* 11, 301–312.
- Schulz, G. E. (2003) Transmembrane  $\beta$ -barrel proteins, *Adv. Protein Chem.* 63, 47–70.
- Popot, J. L., and Engelman, D. M. (2000) Helical membrane protein folding, stability, and evolution, *Annu. Rev. Biochem.* 69, 881–922.
- Henderson, I. R., Navarro-Garcia, F., and Nataro, J. P. (1998) The great escape: structure and function of the autotransporter proteins, *Trends Microbiol.* 6, 370–378.
- Henderson, I. R., Navarro-Garcia, F., Desvaux, M., Fernandez, R. C., and Ala'Aldeen, D. (2004) Type V protein secretion pathway: the autotransporter story, *Microbiol. Mol. Biol. Rev.* 68, 692–744.
- Oomen, C. J., Van Ulsen, P., Van Gelder, P., Feijen, M., Tommassen, J., and Gros, P. (2004) Structure of the translocator domain of a bacterial autotransporter, *EMBO J.* 23, 1257–1266.
- Pohlner, J., Halter, R., Beyreuther, K., and Meyer, T. F. (1987) Gene structure and extracellular secretion of *Neisseria gonorrhoeae* IgA protease, *Nature* 325, 458–462.
- Yen, M. R., Peabody, C. R., Partovi, S. M., Zhai, Y., Tseng, Y. H., and Saier, M. H. (2002) Protein-translocating outer membrane porins of Gram-negative bacteria, *Biochim. Biophys. Acta* 1562, 6–31.
- Benz, I., and Schmidt, M. A. (1992) AIDA-I, the adhesin involved in diffuse adherence of the diarrhoeagenic *Escherichia coli* strain 2787 (O126:H27), is synthesized via a precursor molecule, *Mol. Microbiol.* 6, 1539–1546.
- Suhr, M., Benz, I., and Schmidt, M. A. (1996) Processing of the AIDA-I precursor: removal of AIDA and evidence for the outer membrane anchoring as a  $\beta$ -barrel structure, *Mol. Microbiol.* 22, 31–42.
- Kajava, A. V., Cheng, N., Cleaver, R., Kessel, M., Simon, M. N., Willery, E., Jacob-Dubuisson, F., Loch, C., and Steven, A. C. (2001)  $\beta$ -helix model for the filamentous haemagglutinin adhesin of *Bordetella pertussis* and related bacterial secretory proteins, *Mol. Microbiol.* 42, 279–292.
- Oliver, D. C., Huang, G., Nodel, E., Pleasance, S., and Fernandez, R. C. (2003) A conserved region within the *Bordetella pertussis* autotransporter BrkA is necessary for folding of its passenger domain, *Mol. Microbiol.* 47, 1367–1383.
- Surrey, T., Schmid, A., and Jähnig, F. (1996) Folding and Membrane Insertion of the Trimeric  $\beta$ -Barrel Protein OmpF, *Biochemistry* 35, 2283–2288.
- Struyve, M., Moons, M., and Tommassen, J. (1991) Carboxy-terminal phenylalanine is essential for the correct assembly of a bacterial outer membrane protein, *J. Mol. Biol.* 218, 141–148.
- de Cock, H., and Tommassen, J. (1996) Lipopolysaccharides and divalent cations are involved in the formation of an assembly-competent intermediate of outer-membrane protein PhoE of *E. coli*, *EMBO J.* 15, 5567–5573.
- de Cock, H., van Blokland, S., and Tommassen, J. (1996) *In vitro* insertion and assembly of outer membrane protein PhoE of *Escherichia coli* K-12 into the outer membrane. Role of Triton X-100, *J. Biol. Chem.* 271, 12885–12890.
- de Cock, H., Brandenburg, K., Wiese, A., Holst, O., and Seydel, U. (1999) Non-lamellar structure and negative charges of lipopolysaccharides required for efficient folding of outer membrane protein PhoE of *Escherichia coli*, *J. Biol. Chem.* 274, 5114–5119.
- Surrey, T., and Jahnig, F. (1992) Refolding and oriented insertion of a membrane protein into a lipid bilayer, *Proc. Natl. Acad. Sci. U.S.A.* 89, 7457–7461.
- Surrey, T., and Jahnig, F. (1995) Kinetics of folding and membrane insertion of a  $\beta$ -barrel membrane protein, *J. Biol. Chem.* 270, 28199–28203.
- Kleinschmidt, J. H., and Tamm, L. K. (1996) Folding intermediates of a  $\beta$ -barrel membrane protein. Kinetic evidence for a multi-step membrane insertion mechanism, *Biochemistry* 35, 12993–13000.
- Kleinschmidt, J. H., and Tamm, L. K. (1999) Time-resolved distance determination by tryptophan fluorescence quenching: probing intermediates in membrane protein folding, *Biochemistry* 38, 4996–5005.
- Kleinschmidt, J. H., Wiener, M. C., and Tamm, L. K. (1999) Outer membrane protein A of *E. coli* folds into detergent micelles, but not in the presence of monomeric detergent, *Protein Sci.* 8, 2065–2071.
- Kleinschmidt, J. H., den Blaauwen, T., Driessen, A. J., and Tamm, L. K. (1999) Outer membrane protein A of *Escherichia coli* inserts and folds into lipid bilayers by a concerted mechanism, *Biochemistry* 38, 5006–5016.
- Kleinschmidt, J. H., and Tamm, L. K. (2002) Secondary and Tertiary Structure Formation of the  $\beta$ -Barrel Membrane Protein OmpA is Synchronized and Depends on Membrane Thickness, *J. Mol. Biol.* 324, 319–330.
- Conlan, S., Zhang, Y., Cheley, S., and Bayley, H. (2000) Biochemical and biophysical characterization of OmpG: A monomeric porin, *Biochemistry* 39, 11845–11854.
- Conlan, S., and Bayley, H. (2003) Folding of a Monomeric Porin, OmpG, in Detergent Solution, *Biochemistry* 42, 9453–9465.
- Yadav, S., and Ahmad, F. (2000) A New Method for the Determination of Stability Parameters of Proteins from Their Heat-Induced Denaturation Curves, *Anal. Biochem.* 283, 207–213.
- Matouschek, A., Matthews, J. M., Johnson, C. M., and Fersht, A. R. (1994) Extrapolation to water of kinetic and equilibrium data for the unfolding of barnase in urea solutions, *Protein Eng.* 7, 1089–1095.

32. Benz, I., and Schmidt, M. A. (1989) Cloning and expression of an adhesin (AIDA-I) involved in diffuse adherence of enteropathogenic *Escherichia coli*, *Infect. Immun.* 57, 1506–1511.
33. Tabor, S., and Richardson, C. C. (1985) A bacteriophage T7 RNA polymerase/promoter system for controlled exclusive expression of specific genes, *Proc. Natl. Acad. Sci. U.S.A.* 82, 1074–1078.
34. Suhr, M. (1998) Ph.D. Thesis, University of Münster, Münster, Germany.
35. Schmidt, B., Kromer, M., and Schulz, G. E. (1996) Expression of porin from *Rhodospseudomonas blastica* in *Escherichia coli* inclusion bodies and folding into exact native structure, *FEBS Lett.* 381, 111–114.
36. Miroux, B., and Walker, J. E. (1996) Over-production of proteins in *Escherichia coli*: mutant hosts that allow synthesis of some membrane proteins and globular proteins at high levels, *J. Mol. Biol.* 260, 289–298.
37. Gill, S. C., and von Hippel, P. H. (1989) Calculation of Protein Extinction Coefficients from Amino Acid Sequence Data, *Anal. Biochem.* 182, 319–326.
38. Lakowicz, J. R. (1999) *Principles of Fluorescence Spectroscopy*, Kluwer Academic/Plenum Publishers, New York.
39. Heller, K. B. (1978) Apparent molecular weights of a heat-modifiable protein from the outer membrane of *Escherichia coli* in gels with different acrylamide concentrations, *J. Bacteriol.* 134, 1181–1183.
40. Schweizer, M., Hindennach, I., Garten, W., and Henning, U. (1978) Major proteins of the *Escherichia coli* outer cell envelope membrane. Interaction of protein II with lipopolysaccharide, *Eur. J. Biochem.* 82, 211–217.
41. Sanders, C. R., Kuhn Hoffmann, A., Gray, D. N., Keyes, M. H., and Ellis, C. D. (2004) French swimwear for membrane proteins, *ChemBioChem* 5, 423–426.
42. Eisele, J. L., and Rosenbusch, J. P. (1990) *In vitro* folding and oligomerization of a membrane protein. Transition of bacterial porin from random coil to native conformation, *J. Biol. Chem.* 265, 10217–10220.
43. Schulz, G. E. (2002) The structure of bacterial outer membrane proteins, *Biochim. Biophys. Acta* 1565, 308–317.
44. Pebay-Peyroula, E., Garavito, R. M., Rosenbusch, J. P., Zulauf, M., and Timmins, P. A. (1995) Detergent structure in tetragonal crystals of OmpF porin, *Structure* 3, 1051–1059.
45. Stryer, L. (1965) The Interaction of a Naphthalene Dye with Apomyoglobin and Apohemoglobin. A Fluorescent Probe of Non-polar Binding Sites, *J. Mol. Biol.* 13, 482–495.
46. Tanford, C. (1968) Protein Denaturation, Part A, *Adv. Protein Chem.* 23, 121–217.
47. Fersht, A. R. (1999) *Structure and Mechanism in Protein Science. A Guide to Enzyme Catalysis and Protein Folding*, W. H. Freeman and Co., New York.
48. Pace, C. N. (1990) Conformational stability of globular proteins, *Trends Biochem. Sci.* 15, 14–17.
49. Maurer, J., Jose, J., and Meyer, T. F. (1999) Characterization of the Essential Transport Function of the AIDA-I Autotransporter and Evidence Supporting Structural Predictions, *J. Bacteriol.* 181, 7014–7020.
50. Müller, D. (2003) Diploma Thesis, Westfälische-Wilhelms Universität Münster, Münster, Germany.
51. Buchanan, S. K. (1999) Beta-barrel proteins from bacterial outer membranes: structure, function and refolding, *Curr. Opin. Struct. Biol.* 9, 455–461.
52. Shannon, J. L., and Fernandez, R. C. (1999) The C-terminal domain of the *Bordetella pertussis* autotransporter BrkA forms a pore in lipid bilayer membranes, *J. Bacteriol.* 181, 5838–5842.
53. Rogl, H., Kosemund, K., Kuhlbrandt, W., and Collinson, I. (1998) Refolding of *Escherichia coli* produced membrane protein inclusion bodies immobilised by nickel chelating chromatography, *FEBS Lett.* 432, 21–26.
54. Kleinschmidt, J. H. (2003) Membrane protein folding on the example of outer membrane protein A of *Escherichia coli*, *Cell. Mol. Life Sci.* 60, 1547–1558.
55. Dekker, N., Merck, K., Tommassen, J., and Verheij, H. M. (1995) *In vitro* folding of *Escherichia coli* outer-membrane phospholipase A, *Eur. J. Biochem.* 232, 214–219.
56. Otzen, D. E., and Oliveberg, M. (1999) Salt-induced detour through compact regions of the protein folding landscape, *Proc. Natl. Acad. Sci. U.S.A.* 96, 11746–11751.
57. Otzen, D. E., Kristensen, O., and Oliveberg, M. (2000) Designed protein tetramer zipped together with a hydrophobic Alzheimer homology: a structural clue to amyloid assembly, *Proc. Natl. Acad. Sci. U.S.A.* 97, 9907–9912.
58. Pedersen, J. S., Christensen, G., and Otzen, D. E. (2004) Modulation of S6 fibrillation by unfolding rates and gatekeeper residues, *J. Mol. Biol.* 341, 575–588.
59. Mogensen, J. E., Holm, J., Ipsen, H., and Otzen, D. E. (2004) Elimination of a Misfolded Folding Intermediate by a Single Point Mutation, *Biochemistry* 43, 3357–3367.
60. Ohnishi, Y., Nishiyama, M., Horinouchi, S., and Beppu, T. (1994) Involvement of the COOH-terminal pro-sequence of *Serratia marcescens* serine protease in the folding of the mature enzyme, *J. Biol. Chem.* 269, 32800–32806.
61. Branden, C., and Tooze, J. (1999) *Introduction to Protein Structure*, 2nd ed., Garland Publishing, New York.
62. White, S. H., and Wimley, W. C. (1999) Membrane Protein Folding and Stability: Physical Principles, *Annu. Rev. Biophys. Biomol. Struct.* 28, 319–365.
63. Luckey, M., Ling, R., Dose, A., and Malloy, B. (1991) Role of a disulfide bond in the thermal stability of the LamB protein trimer in *Escherichia coli* outer membrane, *J. Biol. Chem.* 266, 1866–1871.
64. Heinz, C., Engelhardt, H., and Niederweis, M. (2003) The core of the tetrameric mycobacterial porin MspA is an extremely stable  $\beta$ -sheet domain, *J. Biol. Chem.* 278, 8678–8685.
65. Phale, P. S., Philippsen, A., Kiefhaber, T., Koebnik, R., Phale, V. P., Schirmer, T., and Rosenbusch, J. P. (1998) Stability of Trimeric OmpF Porin: The Contributions of the Latching Loop L2, *Biochemistry* 37, 15663–15670.
66. Bonhivers, M., Desmadril, M., Moeck, G. S., Boulanger, P., Colomer-Pallas, A., and Letellier, L. (2001) Stability studies of FhuA, a two-domain outer membrane protein from *Escherichia coli*, *Biochemistry* 40, 2606–2613.
67. Hong, H., and Tamm, L. K. (2004) Elastic coupling of integral membrane protein stability to lipid bilayer forces, *Proc. Natl. Acad. Sci. U.S.A.* 101, 4065–4070.
68. Garcia-Mira, M. M., Boehringer, D., and Schmid, F. X. (2004) The folding transition state of the cold shock protein is strongly polarized, *J. Mol. Biol.* 339, 555–569.
69. Otzen, D. E. (2003) Folding of DsbB in Mixed Micelles: A Kinetic Analysis of the Stability of a Bacterial Membrane Protein, *J. Mol. Biol.* 330, 641–649.
70. Popot, J. L., and Engelman, D. M. (1990) Membrane protein folding and oligomerization: the two-stage model, *Biochemistry* 29, 4031–4037.
71. Whitmore, L., and Wallace, B. A. (2004) DICHROWEB, an online server for protein secondary structure analyses from circular dichroism spectroscopic data, *Nucleic Acids Res.* 32, W668–673.